Age of Information in Random Access Networks with Stochastic Arrivals

Igor Kadota and Eytan Modiano
Laboratory for Information and Decision Systems, MIT
kadota@mit.edu modiano@mit.edu

***Abstract*—We consider a Random Access network with a number of nodes transmitting time-sensitive information to a wireless base station. Packets are generated according to a stochastic process and nodes employ either Slotted-ALOHA or Carrier-Sense Multiple Access (CSMA) to transmit these packets. A packet collision occurs when two or more nodes transmit simultaneously and a successful packet transmission occurs when a node transmits without interference. The goal is to optimize the Random Access mechanism in terms of information freshness, which is captured by the Age of Information (AoI) metric.**

In this paper, we propose a framework to analyze and optimize the average AoI in Random Access networks with stochastic packet generation. In particular, we develop a discrete-time model, derive an approximate expression for the average AoI in the network, and then use this expression to optimize the Random Access mechanism. Furthermore, we implement the optimized Random Access mechanism in a Software Defined Radio testbed and compare the AoI measurements with analytical and numerical results in order to validate our framework. Our approach allows us to evaluate the combined impact of the packet generation rate, transmission probability, and size of the network on the AoI performance.

***Index Terms*—Age of Information, Random Access, Optimization, Wireless Networks, Software Defined Radio testbed**

I. Introduction

Random Access is a multiple access technique that underpins protocols such as *Slotted-ALOHA* and *Carrier-Sense Multiple Access* (CSMA). A main difference between the two protocols is that CSMA utilizes carrier sensing capabilities to avoid packet collisions, while Slotted-ALOHA is a simpler protocol that does not assume that nodes have carrier sensing capabilities.

Random Access networks are widely adopted. Examples of emerging time-sensitive applications that are implemented using Random Access networks are abundant: monitoring mobile ground-robots in automated fulfillment warehouses at Amazon [1], [2] and Alibaba [3]; collision prevention applications [4] for vehicles on the road [5]–[8]; and path planning, localization and motion control for multi-robot formations using drones [9], [10] and using ground-robots [11]. Random Access networks and, in particular, WiFi networks are an attractive choice for they are low-cost, well-established, and immediately available in drones, computing platforms, and sensors. Moreover, as showcased by these various implementations, *small-scale underloaded* Random Access networks are capable of supporting time-sensitive applications.

Two main shortcomings of Random Access networks are *scalability* and *congestion*. In particular, as the size of the network or the congestion level increases, the network becomes overloaded and the information freshness degrades sharply, resulting in outdated information at the destination, which can lead to system failures and safety risks. In this paper, we analyze and optimize information freshness in Slotted-ALOHA and CSMA networks with stochastic packet generation from a finite number of sources.

The literature on the analysis and optimization of Slotted-ALOHA and CSMA networks is vast, dating almost five decades [12]–[14]. For a survey on throughput and delay optimization of CSMA networks, we refer the readers to [15]. The Age of Information (AoI) is a recently proposed [16], [17] performance metric that *captures how fresh the information is from the perspective of the destination.* The optimization of *centralized* multiple access mechanisms in terms of AoI has been considered in numerous works including [18]–[28]. The optimization of *distributed* mechanisms, such as Slotted-ALOHA and CSMA, in terms of AoI has been recently considered in [17], [29]–[36].

The authors of [29]–[31] studied Slotted-ALOHA networks with sources that generate packets on demand. Slotted-ALOHA networks with stochastic packet generation were considered in [32], [33]. In particular, the authors of [32] analyzed Slotted-ALOHA networks in the limit as the number of sources goes to infinity, and proposed a mechanism to dynamically drop packets in order to minimize the average AoI in the network. The authors of [33] used Queueing Theory to analyze AoI in a wireless network with Bernoulli packet arrivals and geometric interdelivery times, and used simulation results to optimize the AoI performance under three classes of multiple access mechanisms, including Slotted-ALOHA.

CSMA networks were considered in [17], [34]–[36]. In particular, the authors of [17] used simulations and experimental results to evaluate the average AoI in a CSMA network. The authors of [34] proposed modifications to the CSMA mechanism inspired by a centralized Whittle's Index scheduling policy, and evaluated the CSMA network using numerical results. The authors of [35] developed a discrete-time model for a CSMA network with sources that generate packets on demand, derived an expression for the average AoI,

This work was supported by NSF Grants AST-1547331, CNS-1713725, and CNS-1701964, and by Army Research Office (ARO) grant number W911NF-17-1-0508.

and then used Game Theory to analyze the coexistence of WiFi and Dedicated Short-Range Communications (DSRC) in terms of throughput and AoI. The authors of [36] developed a continuous-time model for a collision-free CSMA network with stochastic packet generation, derived an expression for the average AoI, and then used this expression to find the optimal back-off rate. Notice that [36] does not consider the effects of packet collisions which, as we see in this paper, play an important role in the AoI optimization of Random Access networks.

Our contributions. In this paper, we propose a framework to analyze and optimize the average AoI in Random Access networks with stochastic packet generation. In particular, we develop a discrete-time network model that accounts for the effects of packet collisions and derive an accurate approximation for the average AoI in the network. We then use the analytical model to optimize the Random Access mechanism in terms of AoI. Our approach allows us to evaluate the combined impact of the packet generation rate, transmission probability, and size of the network on the AoI performance. Finally, we implement the optimized CSMA network in the Software Defined Radio testbed in Fig. 8 and compare the AoI measurements with analytical results and simulations. To the best of our knowledge, this is the first work to provide theoretical results on the optimization of a CSMA network with stochastic packet generation and packet collisions, and the first work to implement a CSMA mechanism optimized for AoI.

The remainder of this paper is organized as follows. In Sec. II, we present the network model. In Sec. III, we derive expressions for the interdelivery interval, packet delay and AoI. In Sec. IV, we optimize the Random Access network in terms of AoI. In Sec. V, we implement the optimized CSMA network and discuss experimental results. This paper is concluded in Sec. VI.

II. System Model

Consider a broadcast single-hop wireless network with N sources transmitting time-sensitive information to the Base Station (BS) using Random Access. Let the time be slotted, with *mini-slot* duration δ seconds and mini-slot index $k \in \{1,2,\cdots,K\}$, where $K\delta$ is the time-horizon of this discrete-time system. At the beginning of every mini-slot k, each source $i \in \{1,2,\cdots,N\}$ generates a new packet with probability $\lambda_i \in (0,1]$. Let $a_i(k)$ be the indicator function that is equal to 1 when source i generates a fresh packet in mini-slot k, and equal to 0, otherwise. The packet generation process is i.i.d. over mini-slots and independent across different sources, with $\mathbb{P}(a_i(k)=1)=\lambda_i$.

Queueing discipline. *Sources keep only the most recently generated packet, i.e. the freshest packet, in their transmission queue.* When source i generates a new packet at the beginning of mini-slot k, older packets are discarded from its transmission queue. This queueing discipline is known to optimize the AoI in a variety of contexts [37]–[39]. Notice that delivering the most recently generated packet provides the freshest information to the BS. Moreover, notice that when a packet with *older information* is delivered after a packet with *fresher information*, the information freshness at the BS is not affected. Hence, discarding *older packets* from the transmission queue when a *fresher packet* is generated has no effect on the information freshness.

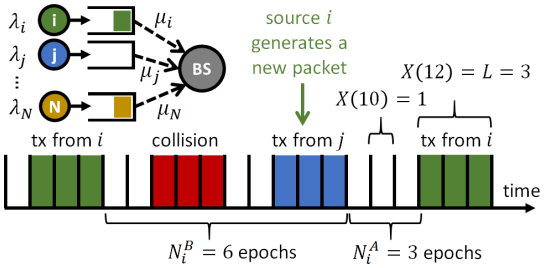

Fig. 1. Illustration of the Random Access network and associated timeline with packet generation, transmission and collision events.

Random Access mechanism. When there is a transmission opportunity in mini-slot k and source i has an undelivered packet, then source i starts transmitting with probability $\mu_i \in (0,1]$, and idles with probability $1-\mu_i$. The mini-slot duration δ is set to the time needed for any source to detect a transmission from other sources. Hence, if source i is the only source to start transmitting in mini-slot k, then all other sources detect the transmission by the beginning of mini-slot $k+1$ and defer new transmissions until source i stops transmitting. As a result, if source i is the only source to start transmitting in mini-slot k, then this transmission is successful. Otherwise, if two or more sources start transmitting in the same mini-slot k, then there is a *packet collision* and the BS is unable to receive these packets. After the collision, sources continue to employ Random Access to retransmit their undelivered packets. The duration of a collision or a successful packet transmission is L mini-slots, as illustrated in Fig. 1. We assume that there are no hidden/exposed sources and that the feedback from the BS is instantaneous and without error.

Definition of epoch. Sources continually sense the wireless channel and defer transmissions until the channel is idle. Transmission opportunities occur when the channel is idle at the beginning of a mini-slot. Denote by *epoch* the time interval between two consecutive transmission opportunities, let $t \in \{1,2,\cdots,T\}$ be the *epoch index*, where T is the total number of epochs, and let $X(t)$ be the number of mini-slots contained in epoch t. It follows that $X(t)=L$ mini-slots when epoch t is busy, i.e. contains a transmission attempt, and $X(t)=1$ mini-slot when epoch t is idle. By dividing the time-horizon into epochs, we obtain $K=\sum_{t=1}^{T} X(t)$. In Fig. 1, we have $K=20$ mini-slots and $T=12$ epochs. Notice that each epoch is associated with a *single* transmission opportunity.

A. Transmission probability

Source i can transmit at the beginning of every *epoch* in which its transmission queue has a packet. Let $q_i(t)$ be the probability of source i transmitting a packet in epoch t. Naturally, if the transmission queue is empty, then $q_i(t)=0$,

and if the transmission queue has a packet, then $q_i(t) = \mu_i$. It follows that the probability of epoch t being idle, containing a successful packet transmission from source i, and containing a packet collision are given by

$$\mathbb{P}^I(t) = \prod_{i=1}^{N}(1-q_i(t))\,; \tag{1a}$$

$$\mathbb{P}_i^S(t) = q_i(t)\prod_{j=1,j\neq i}^{N}(1-q_j(t))\,; \tag{1b}$$

$$\mathbb{P}^C(t) = 1-\mathbb{P}^I(t)-\sum_{i=1}^{N}\mathbb{P}_i^S(t)\,, \tag{1c}$$

respectively. Notice that $\mathbb{P}^I(t)$, $\mathbb{P}_i^S(t)$, and $\mathbb{P}^C(t)$ depend on the state of the transmission queues of every source in the network. For simplicity, and since we do not assume global knowledge of the state of the queues, we approximate the transmission probability in epoch t, $q_i(t)$, by its expected time-average $q_i = \lim_{T\to\infty}\sum_{t=1}^{T}\mathbb{E}[q_i(t)]/T$. Equivalent approximations are employed in various works that analyze Random Access networks, such as [29], [35], [40], [41]. In Secs. III and V, we compare the analytical model with simulation and experimental results, and validate this approximation.

To obtain a closed-form expression for the *transmission probability* q_i, we consider the time interval between two consecutive packet deliveries from source i, and divide this interval into two parts: before and after a new packet generation. Let N_i^B be the number of consecutive *epochs* following the start of the interdelivery interval (i.e., after the successful packet transmission) and preceding the packet generation, and let N_i^A be the number of consecutive *epochs* following the packet generation and preceding the actual packet delivery, as illustrated in Fig. 1. Let $X_i^B(t)$ be the number of mini-slots contained in epoch $t \in \{1,\cdots,N_i^B\}$ within the interval N_i^B, and let $X_i^A(t)$ be the number of mini-slots contained in epoch $t \in \{1,\cdots,N_i^A\}$ within the interval N_i^A. The sequence of packet deliveries from source i is a renewal process and, thus, we can employ the elementary renewal theorem [42, Sec. 5.6] to obtain the following expression for the transmission probability

$$q_i = \frac{(\mathbb{E}[N_i^A]+1)\mu_i}{\mathbb{E}[N_i^B]+(\mathbb{E}[N_i^A]+1)}\,,\forall i\,. \tag{2}$$

Notice that the denominator in (2) represents the expected number of *transmission opportunities* in the interdelivery interval and the numerator in (2) represents the expected number of *transmission opportunities* in which source i has a packet to transmit. The expected number of *mini-slots* in the interdelivery interval is discussed in Sec. III-A.

We define the probability that all nodes *other than i* are idle during an arbitrary epoch t as

$$Q^{-i} = \prod_{j=1,j\neq i}^{N}(1-q_j)\,. \tag{3}$$

Proposition 1. *The expected time-average transmission probability of source i is given by*

$$q_i = \left(\frac{(1-\lambda_i)^L Q^{-i}}{1-(1-\lambda_i)Q^{-i}-(1-\lambda_i)^L(1-Q^{-i})}+\frac{1}{\mu_i}\right)^{-1}. \tag{4}$$

Proof. To obtain the transmission probability in (4), we start by deriving expressions for $\mathbb{E}[X_i^B]$ and $\mathbb{E}[X_i^A]$. Then, we use these expected values, the law of iterated expectations, and the fact that $X_i^B(t)$ are i.i.d. over time to derive expressions for $\mathbb{E}[N_i^B]$ and $\mathbb{E}[N_i^A]$. Finally, we substitute $\mathbb{E}[N_i^B]$ and $\mathbb{E}[N_i^A]$ into (2) to obtain (4). The details are omitted due to the space constraint. □

Notice from (4) that, as expected, $q_i \in (0,\mu_i]$. Moreover, notice that changing the packet generation probability λ_i or the conditional transmission probability μ_i of a particular source i, changes the transmission probability q_j of *all sources in the network*. In particular, changing λ_i or μ_i, changes q_i according to (4). In turn, q_i affects $Q^{-j}, \forall j \neq i$, which affects the transmission probabilities q_j of all sources in the network. The set of functions $\{q_i\}_{i=1}^N$ captures the influence that one source has on other sources in the network. This set of functions is further discussed in Secs. III and IV. Next, we develop a framework for analyzing information freshness.

III. Analysis of Age of Information

In this section, we derive analytical expressions for the interdelivery interval, packet delay and AoI, and then, compare the analysis with simulation results. In Sec. IV, we use this framework to optimize Slotted-ALOHA and CSMA networks in terms of AoI.

A. Interdelivery interval

The sequence of packet deliveries from source i is a renewal process. For this reason, henceforth in this section, we focus on a single interdelivery interval. Consider the interdelivery interval in Fig. 1. Let I_i be the number of *mini-slots* between two consecutive packet deliveries from source i. It follows that

$$\mathbb{E}[I_i] = \mathbb{E}\left[\sum_{t=1}^{N_i^B}X_i^B(t)+\sum_{t=1}^{N_i^A}X_i^A(t)+L\right], \tag{5}$$

where the first and second sums on the RHS of (5) represent the total number of mini-slots in the time intervals N_i^B and N_i^A, respectively.

Proposition 2. *A (tight) lower bound on the expected interdelivery interval is given by*

$$\mathbb{E}[I_i] \geq \frac{(1-\lambda_i)^L}{\lambda_i}+\left(L\,\frac{1-Q^{-i}}{Q^{-i}}+1\right)\frac{1}{\mu_i}+L-1\,. \tag{6}$$

Proof. To obtain the lower bound in (6), we derive expressions for the first and second sums on the RHS of (5). The expected value of the second sum $\sum_{t=1}^{N_i^A}X_i^A(t)$ can be obtained by

employing Wald's equality [42, Sec. 5.5] and then using $\mathbb{E}\left[N_i^A\right]$ and $\mathbb{E}\left[X_i^A(t)\right]$, as follows

$$\mathbb{E}\left[\sum_{t=1}^{N_i^A} X_i^A(t)\right] = \mathbb{E}\left[N_i^A\right]\mathbb{E}\left[X_i^A(t)\right] = \frac{1-\mu_i Q^{-i}}{\mu_i Q^{-i}}\left[\frac{(1-\mu_i)Q^{-i}}{1-\mu_i Q^{-i}} + L\,\frac{1-Q^{-i}}{1-\mu_i Q^{-i}}\right]. \quad (7)$$

Notice that we cannot employ Wald's equality to find an expression for the first sum $\sum_{t=1}^{N_i^B} X_i^B(t)$. This is because the random variables $X_i^B(t)$ and N_i^B are dependent. Recall that packet generation events occur at the beginning of *mini-slots*, as opposed to *epochs*. Hence, if the epoch duration $X_i^B(t)$ increases, the number of epochs until the first packet generation N_i^B decreases. To obtain an approximate expression for the first sum, we use the lower bound $Y_i^B \le \sum_{t=1}^{N_i^B} X_i^B(t)$, where Y_i^B is the number of mini-slots that precede the first packet generation. The probability distribution of Y_i^B is given by

$$\mathbb{P}(Y_i^B = 0) = 1-(1-\lambda_i)^L\,; \quad (8a)$$

$$\mathbb{P}(Y_i^B = k) = (1-\lambda_i)^{L+k-1}\lambda_i, \forall k \in \{1,2,\cdots\}\,, \quad (8b)$$

where (8a) represents the probability of source i generating a new packet while delivering the previous packet or in the first mini-slot after the delivery, and (8b) represent the probability of source i generating a new packet $k+1$ mini-slots after delivering the previous packet. From (8a) and (8b) we obtain the lower bound

$$\mathbb{E}[Y_i^B] = \frac{(1-\lambda_i)^L}{\lambda_i} \le \mathbb{E}\left[\sum_{t=1}^{N_i^B} X_i^B(t)\right]. \quad (9)$$

Substituting (7) and (9) into the interdelivery interval in (5) gives (6). □

Notice that if the packet generation occurs during a busy epoch, as illustrated in Fig. 1, then $Y_i^B \le \sum_{t=1}^{N_i^B} X_i^B(t) \le Y_i^B + L - 1$. Otherwise, if the packet generation occurs during an idle epoch, then $Y_i^B = \sum_{t=1}^{N_i^B} X_i^B(t)$. The approximation $\mathbb{E}[Y_i^B] \approx \mathbb{E}[\sum_{t=1}^{N_i^B} X_i^B(t)]$ simplifies the analysis and is particularly accurate in networks with small value of L and/or low transmission probabilities q_i. In Slotted-ALOHA networks, in which $L=1$, we have $\mathbb{E}[Y_i^B] = \mathbb{E}[\sum_{t=1}^{N_i^B} X_i^B(t)]$ and the lower bound on the interdelivery interval in (6) holds with *equality*. Numerical results in Sec. III-C show that the lower bound in (6) is tight in a wide range of network configurations, including CSMA networks with large L, and is particularly accurate near the point of optimal AoI. Next, we derive an analytical expression for the Age of Information.

B. Age of Information

Consider the interdelivery interval in Fig. 2, and assume that packets are time-stamped upon arrival. Naturally, the higher the time-stamp of a packet, the fresher the information contained in this packet. Let $\tau_i(k)$ be the time-stamp of the *freshest* packet received by the BS from source i at the beginning of mini-slot k. Then, the AoI is defined as $\Delta_i(k) := k - \tau_i(k)$. The AoI captures how fresh the information is from the *perspective of the BS*. The value of $\Delta_i(k)$ increases linearly over time while no packet is received, representing the information at the BS getting older. At the beginning of the mini-slot that follows a packet delivery from source i, the value of $\tau_i(k)$ is updated to the time-stamp of the new packet, and the AoI is reduced to the *packet delay*, namely $\Delta_i(k) = z_i = k - \tau_i(k)$, where z_i is the delay associated with the freshest packet delivered from source i. The evolution of AoI and its relationship with the packet delay are illustrated in Fig. 2.

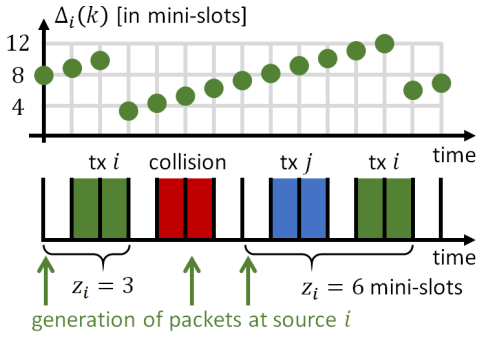

Fig. 2. Timeline with packet generation, transmission and collision events, and associated packet delay z_i and AoI evolution $\Delta_i(k)$.

To capture the Age of Information in the entire network, we define the infinite-horizon expected network AoI (NAoI) as

$$NAoI := \lim_{K\to\infty} \frac{1}{KN}\sum_{k=1}^{K}\sum_{i=1}^{N}\mathbb{E}\left[\Delta_i(k)\right]. \quad (10)$$

Theorem 3. *The expected NAoI is (accurately) approximated by*

$$NAoI \approx \frac{1}{N}\sum_{i=1}^{N}\left(\frac{1-\lambda_i}{\lambda_i} + \left(L\,\frac{1-Q^{-i}}{Q^{-i}}+1\right)\frac{1}{\mu_i}\right) + \frac{1}{2N}\sum_{i=1}^{N}\frac{\frac{(1-\lambda_i)^L}{\lambda_i}\left[\frac{2}{\lambda_i}+L-1\right]-(L-1)\left[\frac{1}{\mu_i}-1\right]}{\left(\frac{(1-\lambda_i)^L}{\lambda_i}+\left(L\,\frac{1-Q^{-i}}{Q^{-i}}+1\right)\frac{1}{\mu_i}+L-1\right)} + \frac{3(L-1)}{2}. \quad (11)$$

Proof. To obtain an expression for the infinite-horizon expected network AoI in (10), we first analyze the evolution of $\Delta_i(k)$ over time, and then we employ tools from Renewal Theory. From Fig. 2, it can be observed that in an interdelivery interval with duration I_i mini-slots and packet delay z_i mini-slots, the value of $\Delta_i(k)$ evolves according to the sequence $z_i, z_i+1, \cdots, z_i+I_i-1$. The sum of AoI in this interdelivery interval is $z_i I_i + I_i(I_i-1)/2$.

The sequence of packet deliveries over time is a renewal process. This fact allowed us to use Renewal Theory to obtain the expression for the transmission probability q_i in (2). However, since the packet delay is not independent across consecutive interdelivery intervals - notice from Fig. 2 that the

value of the packet delay is upper bounded by the previous interdelivery interval - we cannot use Renewal Theory to obtain an expression for NAoI.

To overcome this challenge, we define the *augmented packet delay* $\tilde{z}_i \in \{L, L+1, \cdots\}$, which is unbounded and independent across interdelivery intervals. The augmented packet delay is an upper bound on the packet delay, namely $z_i \leq \tilde{z}_i$, with probability distribution $\mathbb{P}(\tilde{z}_i = L+k) = (1-\lambda_i)^k \lambda_i, k \in \{0,1,\cdots\}$. This upper bound is particularly tight when the interdelivery intervals I_i are large and/or the packet generation probability λ_i is high. Using the elementary renewal theorem for renewal-reward processes [42, Sec. 5.4] and the augmented packet delay $\tilde{z}_i$ into (10), we get

$$\lim_{K\to\infty} \frac{1}{KN} \sum_{k=1}^{K} \sum_{i=1}^{N} \mathbb{E}\left[\Delta_i(k)\right] \leq \frac{1}{N} \sum_{i=1}^{N} \frac{\mathbb{E}[\tilde{z}_i I_i + I_i(I_i-1)/2]}{\mathbb{E}[I_i]}$$
$$= \mathbb{E}[\tilde{z}_i] + \frac{\mathbb{E}[I_i^2]}{2\mathbb{E}[I_i]} - \frac{1}{2}\,. \qquad (12)$$

Substituting the first and second[1] moments of the interdelivery interval, and the first moment of the augmented packet delay into (12), we obtain the approximated expression for NAoI in (11). □

C. Numerical Results

In this section, we consider *symmetric* Random Access networks with $N = 10$ sources, packet generation probabilities $\lambda_i = \lambda, \forall i$, and conditional transmission probabilities $\mu_i = \mu, \forall i$, in four different settings: Slotted-ALOHA networks with $L = 1$ and two values of $\lambda \in \{0.05, 0.5\}$; and CSMA networks with $L = 50$ and two values of $\lambda \in \{0.05, 0.5\}$. We simulate the Random Access networks described in Sec. II, and compare the simulation results with the analytical expressions of the transmission probability q in (4) and NAoI in (11).

In Figs. 3, 4, 5, and 6, we simulate networks with increasing conditional transmission probability $\mu \in (0,1]$. In Figs. 3 and 4, we simulate Slotted-ALOHA networks with packet transmission duration of $L = 1$ mini-slot, and in Figs. 5 and 6, we simulate CSMA networks with $L = 50$. In Figs. 3 and 5, we plot the network AoI, and in Figs. 4 and 6, we plot the transmission probability q. Simulations have a time-horizon of $K = 20 \times 10^6$ mini-slots, each mini-slot with normalized duration $\delta = 1$.

From Figs. 3, 4, 5, and 6, it is evident that the analytical expressions for q and NAoI developed in Secs. II and III, respectively, closely follow the simulation results in a wide range of network configurations, including low and high values of packet transmission duration $L \in \{1, 50\}$, low and high packet generation probabilities $\lambda \in \{0.05, 0.5\}$ and conditional transmission probabilities μ in the interval $(0,1]$.

By comparing Figs. 3 and 5, we can observe that networks with larger packet duration L are less sensitive to changes in the packet generation probability λ. Recall that λ directly affects the number of epochs in which the transmission queue is empty N_i^B and the packet delay z_i. A larger L significantly reduces N_i^B and increases the interdelivery interval I_i, which reduces the impact of N_i^B and z_i on the NAoI performance, thus making the network with larger L less sensitive to variations in λ.

[1] A lower bound on the second moment of the interdelivery interval can be obtained using a similar approach as in Proposition 2.

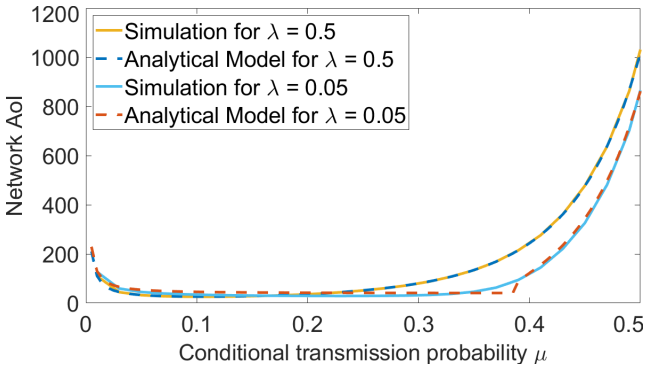

Fig. 3. Simulation of symmetric Slotted-ALOHA networks with $L = 1$, increasing conditional transmission probability μ and two different packet generation probabilities λ.

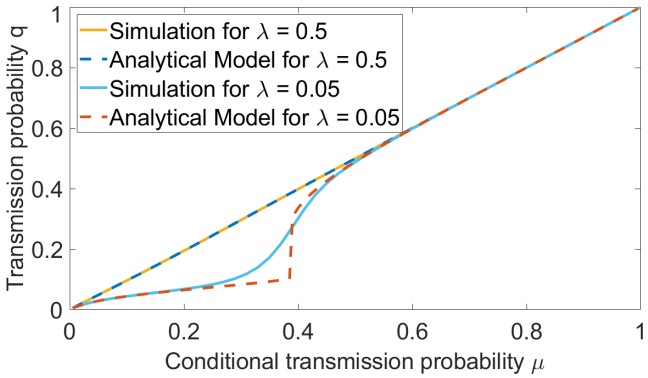

Fig. 4. Simulation of symmetric Slotted-ALOHA networks with $L = 1$, increasing conditional transmission probability μ and two different packet generation probabilities λ.

Figures 3 and 5 also show that: 1) a sub-optimal operating point μ can severely degrade the NAoI performance of the network; and 2) the point of minimum NAoI changes significantly in different network settings. Both observations highlight the importance of optimizing NAoI in Random Access networks, which is addressed in the next section.

Figures 4 and 6 show that for high L and/or high λ, the transmission probability q is comparable to the conditional transmission probability μ, i.e. $q \approx \mu$. In contrast, when λ is low, the relationship between q and μ, which is governed by the *iterated function* $q = g(q, \mu, \lambda)$ in (4), is more involved. Notice that the plot in Fig. 4 for networks with $L = 1$ shows a discontinuity around $\mu = 0.4$ when $\lambda = 0.05$. In turn, for networks with $L = 50$, this discontinuity appears for $\lambda < 0.002$. Figure 7 shows the discontinuity for $\lambda \in \{0.0013, 0.0019\}$. This discontinuity plays an important role in the optimization of NAoI, as we will discuss in Propositions 4 and 6.

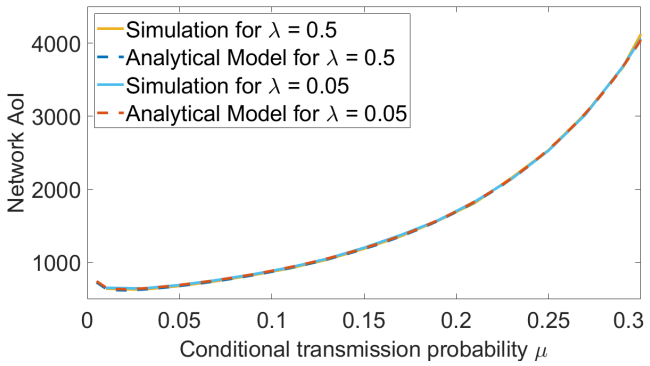

Fig. 5. Simulation of symmetric CSMA networks with $L = 50$, increasing conditional transmission probability μ and two different packet generation probabilities λ.

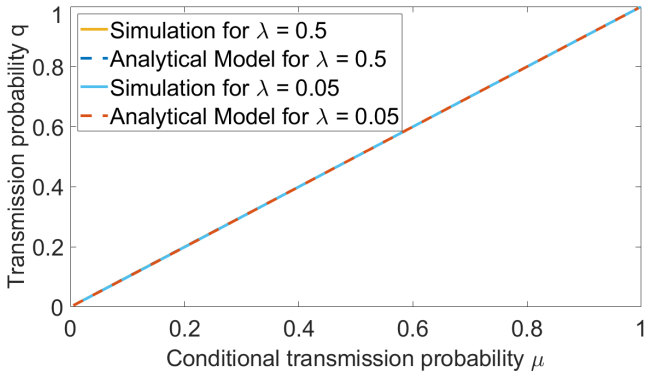

Fig. 6. Simulation of symmetric CSMA networks with $L = 50$, increasing conditional transmission probability μ and two different packet generation probabilities λ.

IV. Network Optimization

In this section, we optimize NAoI in *symmetric* Random Access networks with packet generation probabilities $\lambda_i = \lambda \in (0,1], \forall i$, and conditional transmission probabilities $\mu_i = \mu \in (0,1], \forall i$. In particular, we find the optimal value of μ in terms of the parameters (N, L, λ) for three important cases: 1) Slotted-ALOHA networks, in which $L = 1$; 2) saturated CSMA networks, in which $L > 1$ and packets are generated on demand, i.e. $\lambda = 1$; and 3) general CSMA networks with low packet generation probability $\lambda \ll 1$. Then, we show that the three cases are strongly interconnected. In particular, we show that the results of the third case subsume the results of the first two cases. In Sec. V, we compare the analytical optimization of NAoI with experimental and numerical results.

A. Slotted-ALOHA networks

Consider a symmetric Slotted-ALOHA network. Substituting $L = 1$ into the expression of NAoI in (11), we obtain

$$NAoI \approx \frac{1-\lambda}{\lambda} + \frac{1}{\mu Q} + \frac{\frac{1-\lambda}{\lambda^2}}{\frac{1-\lambda}{\lambda} + \frac{1}{\mu Q}}, \tag{13}$$

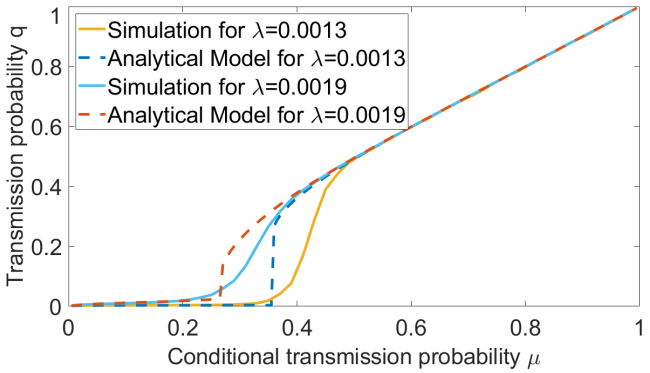

Fig. 7. Simulation of symmetric CSMA networks with $L = 50$, increasing conditional transmission probability μ and two different packet generation probabilities λ.

where $Q = (1-q)^{N-1}$ is the probability that all but one of the nodes are idle during an arbitrary epoch t and q is the transmission probability given by

$$q = \frac{1}{\frac{1-\lambda}{\lambda} Q + \frac{1}{\mu}}. \tag{14}$$

Proposition 4. *In a symmetric Slotted-ALOHA network, the solution candidates $\mu \in (0,1)$ for the NAoI minimization are given by*

$$\mu^{(1)} = \frac{1}{N - \frac{1-\lambda}{\lambda}\left(1 - \frac{1}{N}\right)^{N-1}}; \tag{15a}$$

$$\mu^{(2)} = \frac{q^{(2)}}{1 - \sqrt{1-\lambda}}; \tag{15b}$$

$$\mu^{(3)} = \frac{\left(q^{(3)}\right)^2 (N-1)}{q^{(3)} N - 1}, \tag{15c}$$

where $q^{(2)} \in (0,1)$ and $q^{(3)} \in [1/N, 1)$ are the solutions to the equations below

$$q^{(2)}\left(1 - q^{(2)}\right)^{N-1} = \frac{\lambda}{\sqrt{1-\lambda}}; \tag{16a}$$

$$\left(q^{(3)}\right)^2 \left(1 - q^{(3)}\right)^{N-2} = \frac{\lambda}{(1-\lambda)(N-1)}. \tag{16b}$$

Proof. To find the value of $\mu \in (0,1)$ that minimizes NAoI, we analyze (13). The challenge is that the expression of NAoI in (13) is a function of μ, λ, and q, where q is not directly controllable. The transmission probability q is determined by the *iterated function* $q = g(q, \mu, \lambda)$ in (14). To simplify the expression of NAoI, we substitute (14) into (13), which gives

$$NAoI \approx \frac{1}{q(1-q)^{N-1}} + \frac{1-\lambda}{\lambda^2} q (1-q)^{N-1}, \tag{17}$$

where $q(1-q)^{N-1}$ is the probability of a successful transmission from any given source i.

By analyzing the expression of NAoI in (17) and its partial derivative with respect to q, and then analyzing the iterated function in (14) together with its first and second partial

derivatives, we obtain the solution candidates in (15a)-(15c). Notice that the analysis of the iterated function is non-trivial, since the associated *fixed points* q are not guaranteed to span the entire interval $(0,1)$ due to the discontinuities displayed in Figs. 4 and 7. The complete proof is omitted due to the space constraint. □

Global minimum NAoI. For a given packet generation probability $\lambda \in (0,1]$, we calculate the solution candidates $\mu^{(j)}$, for $j \in \{1,2,3\}$, using (15a)-(16b). Then, we substitute λ and $\mu^{(j)}$ into (14) to find the associated transmission probability q. Finally, by substituting λ, $\mu^{(j)}$ and q into the NAoI expression in (13), we can find and compare the values of NAoI from the different solution candidates. The solution candidate that yields the lowest NAoI is the global minimizer. Notice that this is a low-complexity procedure. Equations (16a) and (16b) have up to four solutions, meaning that the total number of solution candidates from (15a)-(15c) is at most five, for any values of N and λ.

B. Saturated CSMA networks

In this section, we optimize NAoI in symmetric CSMA networks with sources that generate packets on demand, i.e. $\lambda = 1$.

Proposition 5. *In a symmetric CSMA network with $\lambda = 1$, and large values of N and L. The value of μ that minimizes NAoI is given by*

$$\mu^* \approx \frac{1}{N}\sqrt{\frac{2}{L}}\,. \tag{18}$$

Proof. Substituting $\lambda = 1$ into the expression of the transmission probability q in (4), yields $q = \mu$. Taking the partial derivative of NAoI in (11) with respect to μ gives

$$\frac{2(L-1)}{\mu^2} - \frac{2L(1-N\mu)}{\mu^2(1-\mu)^N} + \frac{L(L-1)N(1-\mu)^{N-1}}{(L-(L-1)(1-\mu)^N)^2}\,. \tag{19}$$

Since the first and second terms of the partial derivative in (19) are dominant, especially for CSMA networks with large L, we neglect the third term, equate the partial derivative to zero, and obtain

$$(L-1)(1-\mu)^N = L(1-N\mu)\,, \tag{20}$$

which has a unique solution $\mu^* \in (0, 1/N]$. Then, we approximate $(1-\mu)^N$ in (20) by its second degree Taylor Polynomial to obtain the closed-form solution

$$\mu^* \approx \frac{-N + \sqrt{N^2 + 2(L-1)N(N-1)}}{(L-1)N(N-1)}\,. \tag{21}$$

Notice that when N and L are large, equation (21) is equivalent to (18). □

C. General CSMA networks

In this section, we optimize NAoI in symmetric CSMA networks with low packet generation probability, $\lambda \ll 1$, and then discuss the relationship between the NAoI optimization for general CSMA networks, saturated CSMA networks, and Slotted-ALOHA networks.

Proposition 6. *In a symmetric CSMA network with $\lambda \ll 1$. The solution candidates $\mu \in (0,1)$ for the NAoI minimization are given by*

$$\mu^{(j)} = \left(\frac{1}{q^{(j)}} - \frac{(1-\lambda)^L Q^{(j)}}{1-(1-\lambda)Q^{(j)} - (1-\lambda)^L(1-Q^{(j)})}\right)^{-1}, \tag{22}$$

for $j \in \{1,2,3\}$, where $Q^{(j)} = (1-q^{(j)})^{N-1}$ and $q^{(j)} \in (0,1)$ are the solutions to the equations below

$$(L-1)\left(1-q^{(1)}\right)^N = L\left(1-Nq^{(1)}\right)\,, \tag{23a}$$

$$\left(q^{(2)}\right)^2\left[1-q^{(2)}\right]^{N-2} = \frac{\lambda\left[L-(L-1)\left(1-q^{(2)}\right)^{N-1}\right]^2}{(1-\lambda L)L(N-1)}\,, \tag{23b}$$

and

$$\begin{aligned} &2\lambda^2L^2\left(1-q^{(3)}\right)^2 - 4\lambda^2(L-1)L\left(1-q^{(3)}\right)^{N+2} + \\ &+\left(1-q^{(3)}\right)^{2N}\lambda^2L(L-1)\left(3\left(q^{(3)}\right)^2 - 4q^{(3)} + 2\right) + \\ &-\left(1-q^{(3)}\right)^{2N}\lambda^2 2(L-1)\left(1-q^{(3)}\right)^2 + \\ &+\left(1-q^{(3)}\right)^{2N}\left(q^{(3)}\right)^2(\lambda(L+1)-2) = 0\,. \end{aligned} \tag{23c}$$

Proof. The proof follows similar steps as Proposition 4. The main difference is that the expressions for NAoI in (11) and the iterated function in (4) are more challenging to analyze for CSMA networks than for Slotted-ALOHA networks. To simplify the analysis of (4) and (11) for networks with $\lambda \ll 1$, we use the binomial approximation $(1-\lambda)^L \approx 1-\lambda L$. The complete proof is omitted due to the space constraint. □

Global minimum NAoI. To find the solution candidate $\mu^{(j)}$ that yields the lowest NAoI, we follow the low-complexity procedure described at the end of Sec. IV-A using the results in Proposition 6, the expression for the transmission probability q in (4), and the expression for NAoI in (11). After running this procedure for various network configurations, we observe that *in practice* the candidate $\mu^{(2)}$ associated with (23b) is the minimizer when λ is low, the candidate $\mu^{(1)}$ associated with (23a) is the minimizer when λ is (relatively) high, and the candidate $\mu^{(3)}$ associated with (23c) is never the minimizer. This observation is illustrated in Sec. V-B.

Propositions 4, 5 and 6 determine the optimal value of μ for Slotted-ALOHA networks, saturated CSMA networks with $\lambda = 1$ and general CSMA networks with $\lambda \ll 1$, respectively. Despite these differences, we show that the three propositions are strongly interconnected. In particular, we show that the results in Propositions 4 and 5 are special cases of Proposition 6. Consider (23a)-(23c) from Proposition 6. Notice that when $\lambda = 1$, the equation in (23a) is equivalent to (20) from Proposition 5, and when $L = 1$, the equation in (23a) yields (15a) from Proposition 4. Similarly, it is easy to see that when $L = 1$, the equations in (23b) and (23c) are equivalent to (16b) and (16a) from Proposition 4, respectively.

Hence, the results in Proposition 6 apply not only to CSMA networks with $\lambda \ll 1$, but also to Slotted-ALOHA networks with $\lambda \in (0,1]$, and to CSMA networks with $\lambda = 1$. Thus, we *conjecture that the solution candidates μ for the NAoI minimization given in Proposition 6 are a good approximation to the optimal solution for general Random Access networks with arbitrary parameters (N, L, λ)*. Next, we validate this conjecture by comparing the analytical optimization of NAoI in Proposition 6 with experimental and numerical results.

V. Experimental and Numerical Results

In this section, we describe the experimental setup and then compare the analytical expressions for the NAoI performance (Theorem 3) and NAoI optimization (Proposition 6) with numerical and experimental results. Prior to delving into the details of the experimental setup, we describe the key characteristics of the *optimized CSMA network* that we implemented:

- sources use queues that keep only the freshest packet, as described in Sec. II;
- sources have a conditional transmission probability μ that can be tuned to the optimal value. To adjust the conditional transmission probability to a given $\mu' \in (0,1]$, we set[2] the contention window of the Distributed Coordination Function (DCF) to $W = 2/\mu' - 1$, as proposed in [40, Eq.(8)]; and
- the BS has a time-stamp manager that logs the evolution of $\Delta_i(k)$ over time for every source in the network. Notice that keeping track of $\Delta_i(k) = k - \tau_i(k)$ requires that all nodes in the network are synchronized.

A. Experimental Setup

We implement the *optimized CSMA network* in the FPGA-based Software Defined Radio (SDR) testbed in Fig. 8 composed of one NI USRP 2974 operating as the Base Station, and ten sources: seven NI USRP 2974 and three NI USRP 2953R. The code is developed using a modifiable WiFi reference design [47] with Transport layer based on UDP, MAC layer based on DCF, PHY layer based on the IEEE 802.11n standard with center frequency 2.437 GHz, bandwidth of 20 MHz, mini-slot duration of $\delta = 9\mu$secs, and a fixed MCS index of 5. *We use this WiFi reference design as a starting point, and implement the queueing discipline, the mechanism for adjusting μ, and the time-stamp manager at the FPGA of the SDRs using hardware-level programming.*

B. Results and Discussion

In this section, we evaluate the NAoI performance and optimization using experimental, numerical, and analytical results. We consider a network with $N = 10$ sources, $L = 50$ mini-slots, mini-slot duration of $\delta = 9\mu$secs, and different values of λ and μ, and we compare:

[2]In this paper, we manually set $W = 2/\mu' - 1$. Distributed algorithms that can dynamically tune μ aiming to maximize throughput in CSMA networks were developed in various works including [43]–[46]. Similar algorithms can be used to tune μ for minimizing NAoI. The implementation of such algorithms is out of the scope of this paper.

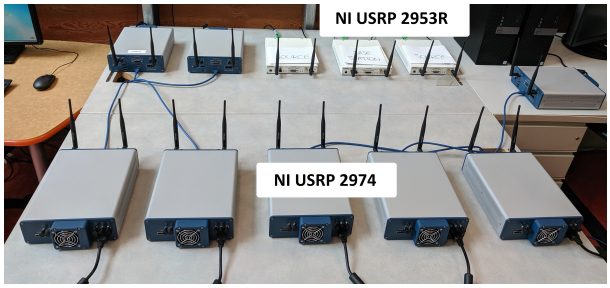

Fig. 8. Software Defined Radio testbed.

TABLE I
NAoI performance (in milliseconds) from the experiments with the SDR testbed, from the simulation results, and from the analytical expression in Theorem 3.

Experimental results						
W	8	16	32	64	128	256
$\lambda = 2.25 \times 10^{-3}$	12.82	6.79	6.77	7.11	8.39	9.10
$\lambda = 4.5 \times 10^{-3}$	25.24	6.89	6.50	7.09	7.82	8.56
$\lambda = 9 \times 10^{-3}$	24.21	8.46	6.89	6.41	7.50	8.79
$\lambda = 45 \times 10^{-3}$	20.87	9.13	6.38	5.98	6.43	7.56
Simulation results						
W	8	16	32	64	128	256
$\lambda = 2.25 \times 10^{-3}$	10.97	6.40	6.18	6.43	6.95	8.73
$\lambda = 4.5 \times 10^{-3}$	20.02	8.45	6.40	5.78	5.93	7.19
$\lambda = 9 \times 10^{-3}$	21.58	8.91	6.62	5.80	5.85	6.96
$\lambda = 45 \times 10^{-3}$	22.93	9.56	6.84	5.81	5.74	6.72
Analytical Model						
W	8	16	32	64	128	256
$\lambda = 2.25 \times 10^{-3}$	11.17	9.54	9.59	9.74	10.03	11.18
$\lambda = 4.5 \times 10^{-3}$	18.35	8.37	6.99	6.70	6.93	8.22
$\lambda = 9 \times 10^{-3}$	21.29	8.99	6.75	5.99	6.04	7.17
$\lambda = 45 \times 10^{-3}$	22.91	9.50	6.84	5.83	5.77	6.72

- **Experimental results**, in which we run the SDR testbed for ten minutes and measure the time-average NAoI as in (10). Each SDR generates packets of 280 bytes with a period of δ/λ seconds and transmits these packets at a rate of approximately $5M$bps, which gives a packet transmission duration of approximately $L = 50$ mini-slots. For each fixed value of $\lambda \in \{2.25, 4.5, 9, 45\} \times 10^{-3}$, we find the optimal μ^* by comparing the values of NAoI for different contention windows $W \in \{8, 16, 32, 64, 128, 256\}$. Recall that $\mu = 2/(W+1)$;
- **Simulation results**, in which we obtain NAoI by simulating the Random Access network described in Sec. II for a time-horizon of $K = 20 \times 10^6$ mini-slots. For each fixed $\lambda \in (0,1)$, we find the optimal μ^* by comparing the values of NAoI for different values of $\mu \in (0,1)$; and
- **Analytical Model**, in which we compute NAoI using Theorem 3 and compute the optimal μ^* associated with a given $\lambda \in (0,1)$ using Proposition 6.

In Table I, we display the NAoI performance from experimental, simulation, and analytical results, for $W \in \{8, 16, 32, 64, 128, 256\}$ and $\lambda \in \{2.25, 4.5, 9, 45\} \times 10^{-3}$. The

results in Table I show that the analytical model closely follows both the simulation and experimental results, and is particularly accurate when λ is large. The lower accuracy of the analytical model for small λ is a result of two approximations: 1) $q(t) \approx q$, introduced in Sec. II-A; and 2) $z \approx \tilde{z}$, introduced in the proof of Theorem 3. Notice that when packet generation is infrequent, i.e. λ is small, the transmission probability in epoch t is often $q(t) = 0$ and the time-averaged transmission probability q can be larger than 0, depending on μ, as illustrated in Figs. 4, 6, and 7, meaning that the approximation $q(t) \approx q$ may be inaccurate. In addition, when λ is small, the packet delay z becomes an important factor in the NAoI analysis, and the upper bound $z \leq \tilde{z}$ becomes less tight. In contrast, when λ is large, which is the *region of interest for the NAoI optimization*, both approximations are accurate.

The transmission probability q of the sources is directly affected by W and λ. In particular, a larger W results in lower μ and q, and a lower λ results in lower q. The results in Table I reflect this relationship and its impact on the NAoI performance. Notice that when the contention window is large, e.g. $W = 256$, the transmission probability is (relatively) low, and NAoI improves for larger λ. In contrast, when the contention window is small, e.g. $W = 8$, the transmission probability is (relatively) large, and NAoI improves for smaller λ. As expected, this behavior is observed in the experimental, simulation, and analytical results.

In Figs. 9 and 10, we display the optimal μ^* and the corresponding minimum $NAoI^*$, respectively, for different values of $\lambda \in (0, 0.05]$. For $\lambda \geq 0.05$, we note that the optimal conditional transmission probability remains constant at $\mu^* = 0.02$ and the value of $NAoI^*$ decreases with λ, achieving $NAoI^* = 5.58$ milliseconds when $\lambda = 1$. The optimal conditional transmission probability μ^* from experimental results is obtained using the measurements in Table I. Figures 9 and 10 show that the analytical results in Secs. III and IV closely follow simulation and experimental results.

In Sec. IV-C, we noted that *in practice* the global minimizer μ^* obtained using Proposition 6 displays a threshold structure. In particular, for each network configuration with parameters (N, L), there exists a threshold $\lambda' \in (0, 1)$ such that, when $\lambda < \lambda'$, the minimizer is the candidate $\mu^{(2)}$ associated with (23b) and, when $\lambda \geq \lambda'$, the minimizer is the candidate $\mu^{(1)}$ associated with (23a). By matching the optimal values of μ^* from the analytical results in Fig. 9 with the solution candidates $\mu^{(j)}$ in Proposition 6, we find that the threshold for $N = 10$ and $L = 50$ is $\lambda' = 0.00187$. This threshold structure was found for various network configurations, and it can be used to reduce the complexity of finding the global minimizer μ^* using Proposition 6. In addition, to further reduce the complexity, we provide an approximate solution for $\mu^{(1)}$. Notice from (22) and (23a) that when λ is high, an approximate solution for $\mu^{(1)}$ and $q^{(1)}$ is given by

$$\mu^{(1)} \approx q^{(1)} \approx \frac{1}{N}\sqrt{\frac{2}{L}} = 0.02\,, \tag{24}$$

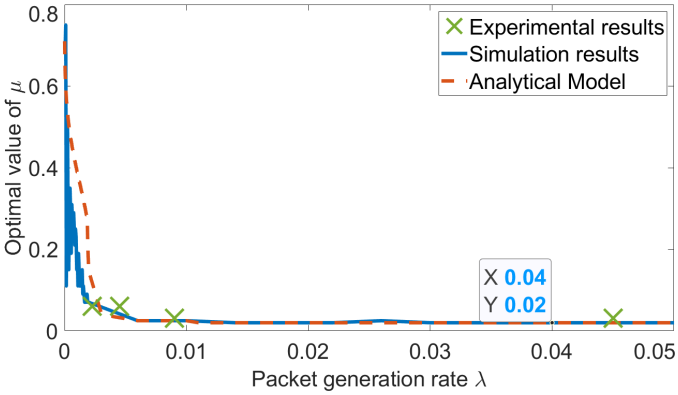

Fig. 9. Optimal conditional transmission probability μ^* obtained from the experiments with the SDR testbed, from the simulation results, and from the analysis in Proposition 6.

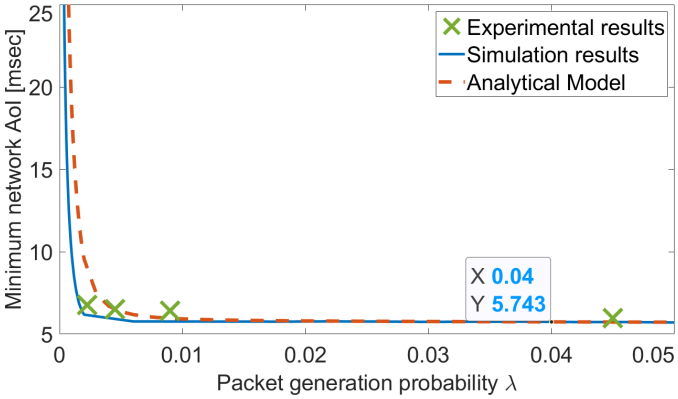

Fig. 10. Optimal NAoI performance associated with the optimal μ^*.

which coincides with μ^* in Fig. 9 for $\lambda > 0.01$.

VI. Summary

In this paper, we studied AoI in networks employing Random Access mechanisms. We considered a wireless network with a number of nodes generating packets according to a Bernoulli process and employing Slotted-ALOHA or CSMA to transmit these packets to the BS. We proposed a framework to analyze and optimize the average AoI in the wireless network. In particular, we developed a discrete-time model and derived expressions for: the time-average transmission probability, a lower bound on the interdelivery interval, an upper bound on the packet delay, and an (accurate) approximation for the average AoI in the network. We then used the analytical expressions to optimize the Random Access mechanism in terms of AoI. Furthermore, we implemented the optimized CSMA network in a Software Defined Radio testbed and compared the AoI measurements with analytical and numerical results in order to validate our framework. We showed that the analytical results accurately track both the simulation and experimental results. Our approach allowed us to evaluate the combined impact of the packet generation rate, transmission probability, and size of the network on the AoI performance.

REFERENCES

[1] P. R. Wurman, R. D'Andrea, and M. Mountz, "Coordinating hundreds of cooperative, autonomous vehicles in warehouses," in *Proceedings of IAAI*, 2007, pp. 1752–1759.

[2] P. Valerio, "Amazon robotics: IoT in the warehouse," online: https://www.informationweek.com/strategic-cio/amazon-robotics-iot-in-the-warehouse/d/d-id/1322366, 2015.

[3] J. Pickering, "Take a look inside Alibaba's smart warehouse where robots do 70% of the work," online: https://www.businessinsider.com/inside-alibaba-smart-warehouse-robots-70-per-cent-work-technology-logistics-2017-9, 2017.

[4] J. B. Kenney, "Dedicated short-range communications (DSRC) standards in the united states," *Proceedings of the IEEE*, vol. 99, no. 7, pp. 1162–1182, 2011.

[5] B. Bloessl, M. Segata, C. Sommer, and F. Dressler, "Performance assessment of IEEE 802.11p with an open source SDR-based prototype," *IEEE Transactions on Mobile Computing*, vol. 17, no. 5, pp. 1162–1175, 2018.

[6] T. T. Almeida, L. de C. Gomes, F. M. Ortiz, J. G. R. Júnior, and L. H. M. K. Costa, "IEEE 802.11p performance evaluation: Simulations vs. real experiments," in *Proceedings of IEEE ITSC*, 2018, pp. 3840–3845.

[7] J. Gozalvez, M. Sepulcre, and R. Bauza, "IEEE 802.11p vehicle to infrastructure communications in urban environments," *IEEE Communications Magazine*, vol. 50, no. 5, pp. 176–183, 2012.

[8] M. Klapez, C. A. Grazia, and M. Casoni, "Application-level performance of IEEE 802.11p in safety-related V2X field trials," *IEEE Internet of Things Journal*, vol. 7, no. 5, pp. 3850–3860, 2020.

[9] E. Ackerman, "This autonomous quadrotor swarm doesn't need GPS," IEEE Spectrum, online: https://spectrum.ieee.org/automaton/robotics/drones/this-autonomous-quadrotor-swarm-doesnt-need-gps, 2017.

[10] J. Alonso-Mora, E. Montijano, T. Nägeli, O. Hilliges, M. Schwager, and D. Rus, "Distributed multi-robot formation control in dynamic environments," *Autonomous Robots*, vol. 43, p. 1079–1100, 2019.

[11] P. Urcola, M. T. Lázaro, J. A. Castellanos, and L. Montano, "Cooperative minimum expected length planning for robot formations in stochastic maps," *Robotics and Autonomous Systems*, vol. 87, pp. 38–50, 2017.

[12] N. Abramson, "THE ALOHA SYSTEM: another alternative for computer communications," in *Proceedings of the Fall Joint Computer Conference*, ser. AFIPS '70 (Fall), 1970, p. 281–285.

[13] L. Kleinrock and F. Tobagi, "Packet switching in radio channels: Part I - carrier sense multiple-access modes and their throughput-delay characteristics," *IEEE Transactions on Communications*, vol. 23, no. 12, pp. 1400–1416, 1975.

[14] L. G. Roberts, "ALOHA packet system with and without slots and capture," *ACM SIGCOMM Computer Communication Review*, vol. 5, no. 2, p. 28–42, 1975.

[15] S.-Y. Yun, Y. Yi, J. Shin, and D. Y. Eun, "Optimal CSMA: A survey," in *Proceedings of ICCS*, 2012, pp. 199–204.

[16] S. Kaul, R. D. Yates, and M. Gruteser, "Real-time status: How often should one update?" in *Proceedings of IEEE INFOCOM*, 2012, pp. 2731–2735.

[17] S. Kaul, M. Gruteser, V. Rai, and J. Kenney, "Minimizing age of information in vehicular networks," in *Proceedings of IEEE SECON*, 2011, pp. 350–358.

[18] Q. He, D. Yuan, and A. Ephremides, "Optimizing freshness of information: On minimum age link scheduling in wireless systems," in *Proceedings of IEEE WiOpt*, 2016.

[19] I. Kadota, A. Sinha, and E. Modiano, "Optimizing age of information in wireless networks with throughput constraints," in *Proceedings of IEEE INFOCOM*, 2018.

[20] C. Joo and A. Eryilmaz, "Wireless scheduling for information freshness and synchrony: Drift-based design and heavy-traffic analysis," in *Proceedings of IEEE WiOpt*, 2017.

[21] R. Talak, S. Karaman, and E. Modiano, "Optimizing information freshness in wireless networks under general interference constraints," in *Proceedings of ACM MobiHoc*, 2018.

[22] R. Talak, I. Kadota, S. Karaman, and E. Modiano, "Scheduling policies for age minimization in wireless networks with unknown channel state," in *Proceedings of IEEE ISIT*, 2018.

[23] Y.-P. Hsu, E. Modiano, and L. Duan, "Age of information: Design and analysis of optimal scheduling algorithms," in *Proceedings of IEEE ISIT*, 2017.

[24] R. D. Yates, P. Ciblat, A. Yener, and M. Wigger, "Age-optimal constrained cache updating," in *Proceedings of IEEE ISIT*, 2017.

[25] I. Kadota, A. Sinha, E. Uysal-Biyikoglu, R. Singh, and E. Modiano, "Scheduling policies for minimizing age of information in broadcast wireless networks," *IEEE/ACM Transactions on Networking*, 2018.

[26] V. Tripathi and S. Moharir, "Age of information in multi-source systems," in *Proceedings of IEEE Globecom*, 2017.

[27] Y. Sun, E. Uysal-Biyikoglu, and S. Kompella, "Age-optimal updates of multiple information flows," in *IEEE INFOCOM workshop on the Age of Information*, 2018.

[28] N. Lu, B. Ji, and B. Li, "Age-based scheduling: Improving data freshness for wireless real-time traffic," in *Proceedings of ACM MobiHoc*, 2018.

[29] H. Chen, Y. Gu, and S.-C. Liew, "Age-of-information dependent random access for massive IoT networks," in *IEEE INFOCOM workshop on the Age of Information*, 2020.

[30] R. Talak, S. Karaman, and E. Modiano, "Distributed scheduling algorithms for optimizing information freshness in wireless networks," in *Proceedings of IEEE SPAWC*, 2018.

[31] S. Kaul and R. D. Yates, "Status updates over unreliable multiaccess channels," in *Proceedings of IEEE ISIT*, 2017.

[32] X. Chen, K. Gatsis, H. Hassani, and S. S. Bidokhti, "Age of information in random access channels," in *Proceedings of IEEE ISIT*, 2020.

[33] A. Kosta, N. Pappas, A. Ephremides, and V. Angelakis, "Age of information performance of multiaccess strategies with packet management," *Journal of Communications and Networks*, vol. 21, no. 3, pp. 244–255, 2019.

[34] Z. Jiang, B. Krishnamachari, S. Zhou, and Z. Niu, "Can decentralized status update achieve universally near-optimal age-of-information in wireless multiaccess channels?" in *Proceedings of IEEE ITC*, vol. 1, 2018, pp. 144–152.

[35] S. Gopal and S. Kaul, "A game theoretic approach to DSRC and WiFi coexistence," in *Proceedings of IEEE INFOCOM workshop on the Age of Information*, 2018.

[36] A. Maatouk, M. Assaad, and A. Ephremides, "On the age of information in a CSMA environment," *IEEE/ACM Transactions on Networking*, vol. 28, no. 2, pp. 818–831, 2020.

[37] M. Costa, M. Codreanu, and A. Ephremides, "On the age of information in status update systems with packet management," *IEEE Transactions on Information Theory*, vol. 62, no. 4, pp. 1897–1910, 2016.

[38] S. Kaul, R. D. Yates, and M. Gruteser, "Status updates through queues," in *Proceedings of IEEE CISS*, 2012.

[39] A. M. Bedewy, Y. Sun, and N. B. Shroff, "The age of information in multihop networks," *IEEE/ACM Transactions on Networking*, vol. 27, no. 3, pp. 1248–1257, 2019.

[40] G. Bianchi, "Performance analysis of the IEEE 802.11 distributed coordination function," *IEEE Journal on Selected Areas in Communications*, vol. 18, no. 3, pp. 535–547, 2000.

[41] Byung-Jae Kwak, Nah-Oak Song, and L. E. Miller, "Performance analysis of exponential backoff," *IEEE/ACM Transactions on Networking*, vol. 13, no. 2, pp. 343–355, 2005.

[42] R. G. Gallager, *Stochastic Processes: Theory for Applications*. Cambridge University Press, 2013.

[43] G. Bianchi and I. Tinnirello, "Kalman filter estimation of the number of competing terminals in an IEEE 802.11 network," in *Proceedings of IEEE INFOCOM*, vol. 2, 2003, pp. 844–852.

[44] I. Kadota, A. Baiocchi, and A. Anzaloni, "Kalman filtering: estimate of the numbers of active queues in an 802.11e EDCA WLAN," *Elsevier Computer Communications*, 2014.

[45] M. Heusse, F. Rousseau, R. Guillier, and A. Duda, "Idle sense: An optimal access method for high throughput and fairness in rate diverse wireless LANs," in *Proceedings of ACM SIGCOMM*, 2005, pp. 121–132.

[46] Y. Grunenberger, M. Heusse, F. Rousseau, and A. Duda, "Experience with an implementation of the idle sense wireless access method," in *Proceedings of ACM CoNEXT*, 2007.

[47] N. Instruments, "LabVIEW communications 802.11 application framework 3.0," online: http://www.ni.com/manuals/, 2019.